



State-of-the-Art Modeling and Simulation of the Brain's Response to Mechanical Loads

Towards Identification of Correspondence Rules to Relate Traumatic Brain Injury in Different Species

ROBERT N. SAUNDERS ,¹ X. GARY TAN,¹ SIDDIQ M. QIDWAI,² and AMIT BAGCHI¹

¹U.S. Naval Research Laboratory, 4555 Overlook Ave SW, Washington, DC 20375, USA; and ²National Science Foundation, 2415 Eisenhower Avenue, Alexandria, VA 22314, USA

(Received 29 June 2018; accepted 16 October 2018; published online 21 November 2018)

Associate Editor Matthew B. Panzer oversaw the review of this article.

Abstract—Traumatic brain injury analysis in humans is exceedingly difficult due to the intrusive methods by which data can be collected; thus, many researchers commonly implement animal surrogates. However, ethical concerns and cost limit the scope of these tests on animal subjects too. Computational models, which provide an alternative method to data collection, are not constrained by these concerns and are able to generate significant amounts of data in relatively short time. This paper shows how the data generated from models of a human and pig head can be used towards developing interspecies correspondence rules for blast overpressure effects. The blast overpressure is simulated using an explosive of known weight and standoff distance and injury is evaluated using criteria in published literature. Results indicate that equivalent blasts in the human and pig produce significantly different injuries, and when equating total injured brain volume, the locations of injury in the brain vary between the species. Charge weight and total injured brain volume are related using a linear regression of the data such that a known injury in the pig or known blast can be used to predict injury or the blast experienced by a human, thus creating a correspondence between the species.

Keywords—Finite element, Blast analysis, Biomechanics, Porcine, Interspecies, Scaling, Injury analysis.

INTRODUCTION

Blast-induced traumatic brain injury (bTBI) has been a significant contributor of warfighter injuries in combat theaters as well as civilian injuries stemming from suicide bombers and other terrorism incidents. However, the exact mechanism of brain injury from a blast overpressure or a shock front is not clearly understood, but it is postulated that pressure in the brain leads to the injury.^{1,8} To explain the causes and/or indicators of bTBI, researchers have been utilizing both experimental and computational approaches to study human and animal subjects, where animals are used as available substitutes for humans. The computational approach utilizes finite element (FE) models of humans and animals, such as pigs, rats, and mice, to assess the impact of blast effects using mechanical variables such as stress and strain, as well as to validate computational models against experimental data.¹⁰ The experimental approach has mostly been to use animal subjects, chiefly murine and porcine subjects, in blast and shock tube tests, and analyze their behavioral responses and subsequent biological assays of the brain from necropsy.¹²

The main objective of these experiments is to relate the changes in behavioral responses to indicators from the biological assays.⁶ However, most of these studies have not come to a consensus on how results should be correlated or interpreted. Similarly, although a large amount of injury data is available from animal subject testing from blast overpressure insult, blunt or projectile impacts,¹² these data have not been applied to interpreting or predicting traumatic brain injury (TBI) in humans, as there is no accepted method to map the findings from animal testing to the human brain injury.

Address correspondence to Amit Bagchi, U.S. Naval Research Laboratory, 4555 Overlook Ave SW, Washington, DC 20375, USA. Electronic mails: robert.saunders@nrl.navy.mil, gary.tan@nrl.navy.mil, sqidwai@nsf.gov, amit.bagchi@nrl.navy.mil

This material is declared a work of the U.S. Government and is not subject to copyright protection in the United States. Approved for public release; distribution is unlimited.

SMQ participates in his personal capacity. Any opinion, findings, and conclusions or recommendations expressed in this material are those of the author and do not necessarily reflect the views of the National Science Foundation.

To formalize the mapping or correspondence between various species, allometric scaling rules generally attempt to establish a relationship between the mass of the brain, head, or body with respect to the injury or survivability from an insult.³⁰ More recent work has attempted to move beyond simple mass-based scaling rules to establish rules based on more complex measures such as impedance mismatch between the different components in the head.¹¹ The work done by Panzer *et al.*¹⁷ provides a summary of the approaches to develop a scaling law or a correspondence rule between humans and animal subjects either experimentally or computationally. As indicated by Panzer *et al.*, new techniques are needed to develop a correlation between the animal subject data (computational or experimental) such that the results can lead to human injury prediction for both concussive and sub-concussive (or mild traumatic brain) injuries.

The aim of this paper is to introduce correspondence rules (i.e., a framework to relate the injuries) between a human and a pig impacted by shock wave loading from a blast simulated using FE modeling. To accomplish this goal, the extent of brain injury is assessed for a given set of side-on blast insults to the subjects utilizing one or more injury criteria in published literature. Injured volumes and locations of the brain are compared for various levels of overpressures to develop correspondence rules between the species.

MATERIALS AND METHODS

The FE model in this work for the human is a 25-year-old Caucasian male representing a 50th percentile U.S. male, 1.8 m tall and weighing 81 kg; while the FE model for the pig is a 6-month-old male Yucatan pig with a length of approximately 900 mm and a weight of 30 kg.⁷ Both the human and porcine models in this work consist of only the head and the neck. A full body porcine model has been developed to more accurately model the pig but due to the computational cost of the full body model, this study is limited to modeling only the head.

Magnetic resonance imaging (MRI) was used to obtain the *in vivo* geometry of both the human and pig heads. The human scans were performed with a 1 mm isotropic resolution and the pig scans used a 0.8 mm isotropic resolution. These high-resolution scans were able to place the necessary emphasis on details in the head and brain. For the human model, the MRI scans were supplemented by computer aided design (CAD) representations of the other components such as the face and neck musculature that could not be differentiated well using the MRI scans alone.^{7,27} The pig MRI scans were supplemented with $0.6 \times 0.6 \times 1.0 \text{ mm}^3$

resolution computed tomography (CT) scans to image the portions which could not be seen in the MRI scans. The MRI, CT, and CAD data were all imported into ScanIP by Simpleware, Inc. (Synopsys[®], Mountain View, USA), and semi-automatically segmented to construct 3-D models of both subjects. All major anatomical regions included in the models of the human and pig heads (Fig. 1) are listed in the first column of Table 1 along with the constitutive model used to represent their mechanical behavior in the second column.

The segmented 3-D models were converted to FE meshes using a multi-part surface decimation algorithm followed by a mixed Delaunay Advancing Front approach, using the Simpleware software.^{7,27} Both models are meshed entirely by solid tetrahedral elements using a modified average nodal pressure formulation.² A tetrahedral mesh was chosen for its ability to better capture the complex geometric features in human and pig brains.^{7,19} An in-house convergence study based on a 1 cm thick sagittal slice of the human head from the same model used in this study subjected to a blast overpressure was carried out to determine the average element size for meshing. The slice was meshed with three levels of refinement. Based on the results of the study, an average element critical length of $\sim 1 \text{ mm}$ was chosen, which guided the software's automated mesh generator. The resulting FE model consists of approximately 4.6 million elements. Approximately, 4000 or less than 0.09% of these elements have poor element quality, which can be monitored for quality control.

The constitutive models for the components of the pig and human are based on available data in the literature considering a range of strain rate tests covering large deformation.⁴ Although there may be differences in porcine and human brain tissue properties, the pig and human components are modeled with the same respective constitutive behaviors due to a lack of data in the literature.²⁵ To capture the mechanical behavior of biological materials subjected to high strain rates and large deformations, the use of non-linear, rate-dependent constitutive formulations is required. The constitutive models chosen for the human and pig models of this work are summarized in Table 1; complete details of the models and calibration process are provided in Brewick *et al.*⁴ It should be noted that mechanical damage is not included in the constitutive models.

Both FE models are implemented and simulated within the CoBi finite element solver.²² Both heads are fixed at the neck. Validation of both models has been completed using blunt impact tests¹⁹ from literature for the human, and blast experiments²³ from literature for the pig.

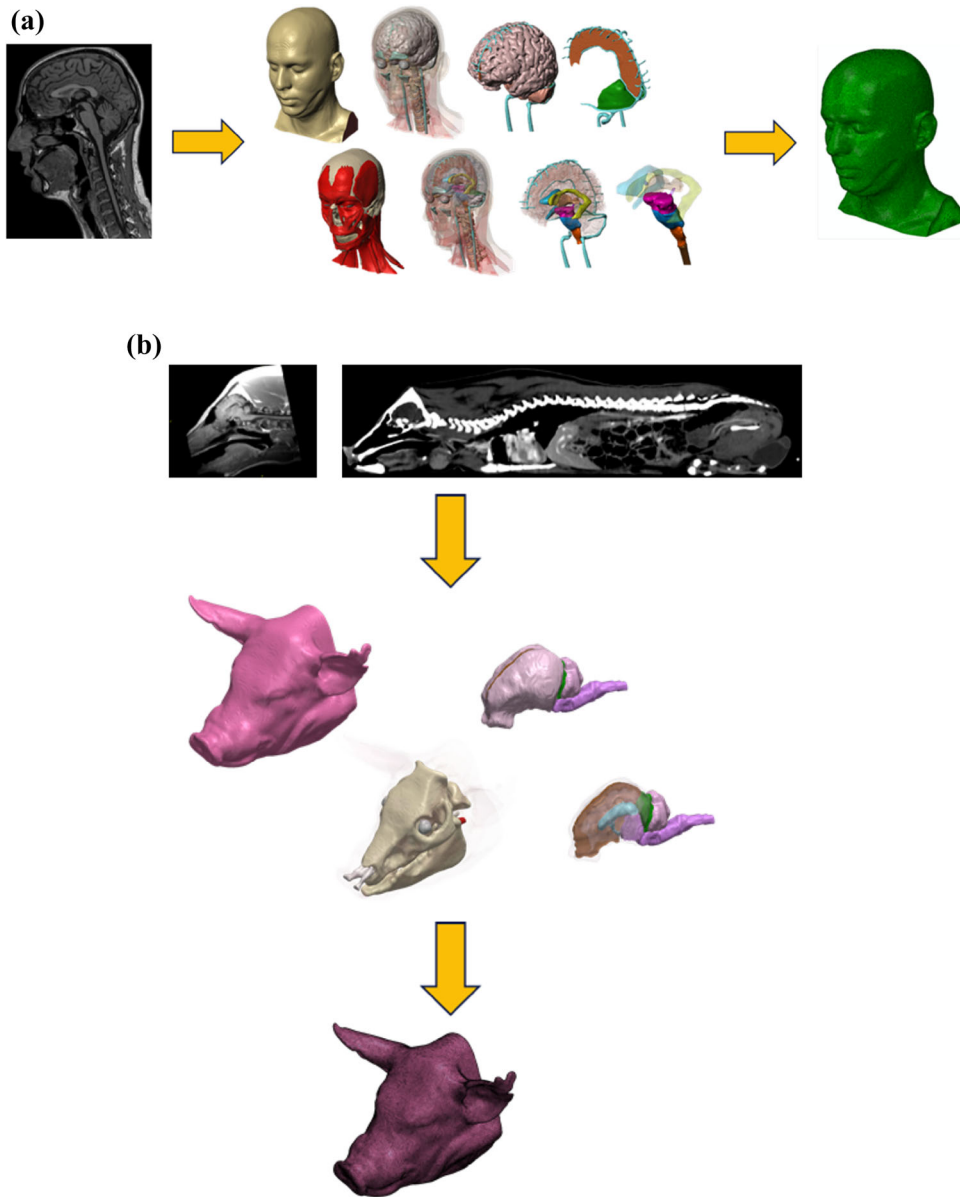


FIGURE 1. (a) Left: high-resolution MRI scan of 50% percentile Caucasian male used to generate human FE model, middle: surface representations of high fidelity human model components after segmentation, right: human model as meshed for implementation in an FE solver. (b) Top: high-resolution full body CT scan (left) and head MRI scan (right) of Yucatan pig used to generate pig FE model, middle: Surface representations of pig model components after segmentation, bottom: pig model as meshed for implementation in an FE solver.

Correspondence Rules Study

To develop correspondence rules to relate TBI in one species to another, the models of both species must be simulated and post-processed in an identical manner so that the only difference that exists is the geometry. To this end, this work subjects the human and the pig heads to identical ConWep blast overpressure loadings.¹⁴ The ConWep model is incorporated into the CoBi FE solver and is used to apply the blast loading on the subjects from a spherical free-field explosion in air (without the ground effect) of a bare

high explosive charge detonated at a distance of 2.7 m from the subjects. At this distance, the time duration of positive phase overpressure for all simulated cases ranges from 2.56 to 2.73 ms. This positive phase duration is approximately what has been observed in free-field blast experiments conducted by the Naval Research Laboratory (NRL). The ConWep pressure time-history is used as the input to the FE models and is referenced in the remainder of this work by the TNT-equivalent charge weight of the detonated explosive. A schematic of the setup is shown in Fig. 2.

TABLE 1. Human and pig anatomical structures included in the FE models and their corresponding constitutive model functional forms.

Component	Constitutive model functional form
Sinus—frontal	Equation of state (Ideal Gas Law)
Sinus—maxillary	
Airway	
Cerebrospinal fluid (CSF)	Hyperelastic (neo-Hookean)
Ventricles—lateral	
Ventricles—third	
Ventricles—fourth	
Ventricles—aqueduct of sylvius	
Ventricles—foramen of Monro	
Venous sinuses and bridging veins	
Eyes (vitreous)	Hyperelastic (neo-Hookean)
Venous sinus and bridging vein walls (shell section)	Anisotropic Hyperelastic (Holzapfel)
Pia mater (shell section)	Hyperelastic (Ogden)
Dura mater (shell section)	Hyperelastic (Ogden)
Falx cerebri	Hyperelastic (Ogden)
Tentorium cerebella	Hyperelastic (Ogden)
Sclera\cornea (shell section)	Hyperelastic (Ogden)
Intervertebral discs	Hyperelastic (Mooney-Rivlin) Hyperelastic (Ogden)
Skull—cortical	Transversely Isotropic Viscoelastic (Prony Series)
Skull—cancellous	Transversely Isotropic Viscoelastic (Prony Series)
Mandible	Transversely Isotropic Viscoelastic (Prony Series)
Vertebrae	Viscoelastic (Prony Series) Viscoelastic (Prony Series) Viscoelastic (Prony Series)
Cerebrum—grey matter	Hyper-viscoelastic (Ogden, Prony series)
Cerebellum—grey matter	
Cerebrum—white matter	
Cerebellum—white matter	
Brain Stem—medulla	
Brain Stem—midbrain	
Brain Stem—pons	
Optic nerves	
Skin	Hyperelastic (Ogden)
Muscles	Hyper-viscoelastic (Ogden, Prony series)
Soft tissue (adipose)	Hyperelastic (Ogden)

Note that not all components are present in both models and components that are in both models share the same constitutive model parameters. See Brewick *et al.*⁴ for detailed model descriptions and calibrations. Grouped materials share the same constitutive model parameters due to similarities in the material.

The results of each FE simulation produce spatially- and temporally-resolved stress-strain data for the whole model that can be compared to biomechanical thresholds for injury criteria suggested in the literature (Table 2) to determine if TBI has occurred. All criteria listed in Table 2 are simultaneously applied on an element-by-element basis to the brain at every time step in the analysis. If an element pressure, shear stress, or shear strain crosses any biomechanical threshold, the element is considered to have been “injured”. Note that the accuracy and validity of these thresholds are not the scope of this paper, and these can be improved as more accurate criteria are developed. Many of the biomechanical injury thresholds can be ignored for a

given analysis due to the redundancy of the criteria or the criteria not being activated. A variable with multiple suggested thresholds can be triggered but it serves no benefit to present the lower threshold results, as they have obviously been triggered.

Toward the objective of developing interspecies correspondence rules, this work considers two tasks: (1) analyze the human and porcine subjects using the same TNT-equivalent overpressure loads to assess the differences in tolerance to blast, and (2) determine the TNT-equivalent loads that produce similar levels of injury in terms of volume in human and porcine subjects. Task 1 will be referred to as the “equal charge weight study” and task 2 will be referred to as the

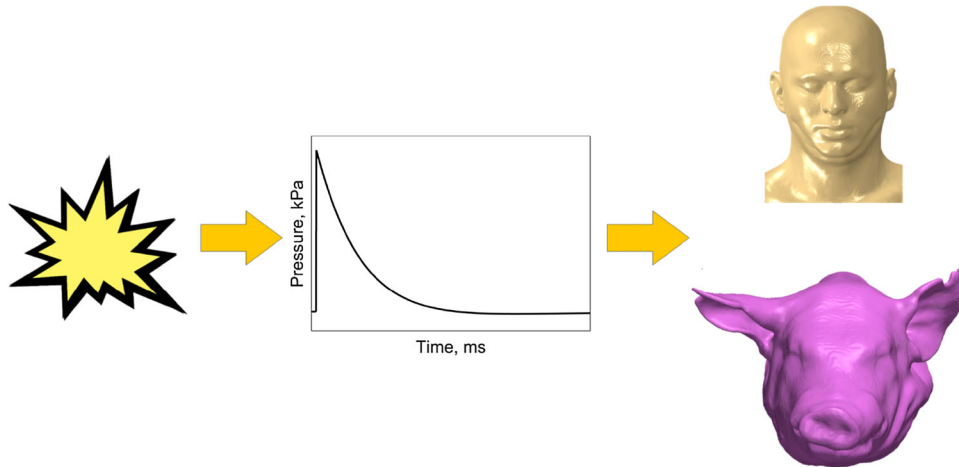


FIGURE 2. Description of applied blast loading (left to right): an explosive is detonated, creating a pressure pulse with known time history, which is then applied to the human and pig models in the side-on orientation.

TABLE 2. Biomechanical thresholds of traumatic brain injury suggested by various authors.

Metric	Limit	Injury	Source
Pressure (kPa)	173	Mild TBI	Ref. 29
	235	Severe TBI	
	- 100	50% probability of concussion (DDM)	Ref. 20
Effective (von Mises) stress (kPa)	11	Severe TBI	Ref. 13
	26	50% probability of mild DAI	Ref. 9
	33	50% severe DAI	
Shear (Tresca) stress (kPa)	7.8	50% probability of mild TBI	Ref. 29
Maximum principal strain (%)	5	Moderate DAI	Ref. 16
	15	50% probability of DAI (CSDM)	Ref. 20
	18	DAI	Ref. 26
	20	50% probability of mild TBI	Ref. 29
	21	50% probability of mild DAI	Ref. 15
	26	50% probability of mild DAI	
Effective (von Mises) strain (%)	25	50% probability of mild DAI	Ref. 9
	35	50% probability of severe DAI	

DDM dilatational damage measure, DAI diffuse axonal injury, CSDM cumulative strain damage measure.

“equal injury study”. In both tasks, the insult-injury correlation will be analyzed by comparing and contrasting the load required to produce a certain level of injury, spatial injury patterns, and temporal injury evolution to potentially develop correspondence rules. The TNT-equivalent loads used for each model in both tasks are summarized in Table 3.

RESULTS

Before considering either task, both FE models were examined under the maximum explosive charge weights used in either types of study (2.0 kg for the human and 4.2 kg for the pig) to determine which injury criteria could be neglected ($< 1\%$ total injured brain volume). The results of the analysis showed that

TABLE 3. ConWep TNT-equivalent loads in kg used in tasks 1 and 2.

Human	Pig
Task 1: equal charge weight Study	
1.4	1.4
1.6	1.6
1.8	1.8
2.0	2.0
Task 2: equal injury study	
1.4	2.3
1.6	2.7
1.8	3.3
2.0	4.2

only pressure-based criteria (173, 235, and - 100 kPa) were being triggered and yielding injured volumes greater than 1%. It should be noted that other criteria

did yield non-zero (< 1%) injured volumes, but were neglected because their values are considered to be within the uncertainty threshold involved in creating the model (i.e., errors in geometric tolerances from MRI scans, FE mesh discretization, and constitutive model calibration propagating through the analyses).^{5,24} Also, note that cavitation in the presence of tensile stress is not considered; that effect is beyond the scope of this work. Based on a careful review of the results, only 235 kPa (severe TBI²⁹) and – 100 kPa (50% probability of concussion, dilatational damage measure¹⁸) pressure-based injury criteria will be shown for the remainder of the work. The results using 173 kPa criterion are not shown as it serves limited purpose to show a lower positive pressure criterion (173 kPa) when a higher threshold (235 kPa) is triggered, despite the possibility that some regions may experience pressure greater than 173 kPa and less than 235 kPa causing differences in quantitative outcome. The results of the maximum load analysis also showed that, due to the nature of stress wave propagation in the head, pressure-based injury had an initial rise (corresponding to the peak pressure passing through the head) and then does not increase for the 30 ms duration of the analysis. Consequently, time history data is only shown up to 0.8 ms of simulation in this work.

In the equal charge weight study, time histories of the injury evolution in the pig and human are shown in Figs. 3a and 3b. A number of features can be immediately identified from these plots. First, the pig appears to have a higher tolerance to blast for the positive pressure criterion but not for the negative pressure criterion, relative to the human. Next, it can be noted that the volume percentage of the brain affected for the human model using the negative pressure injury prediction is substantially lower (nearly a full order of magnitude) than the prediction based on the positive pressure criterion. Finally, it can be observed that the increase in injury over time in the pig and human for both the positive and negative pressure criteria is not linear as was expected based on the non-linear input pressure profile.

The non-linear rise in injury with time is investigated by collecting injured volume data in different regions of the brain at various discrete time steps during the analysis. The results are shown in Figs. 3c–3f for the case of the 2.0 kg blast for both human and pig, where the temporal evolution of injured brain volume is broken down into the total brain volume, and the volumes of the cerebrum, cerebellum, and brain stem. The spatial evolution of injury can also be seen for both the positive and negative pressure criteria in Fig. 4. As expected, the positive pressure injury occurs first on the coup side and then on the counter-

coup side. The negative pressure has the inverse of this behavior, as expected. The geometry of the brain also influences where and when the injury occurs. For the human, the positive pressure injury has a relatively linear increase with time in all three primary brain regions, influencing the nearly linear increase seen in Fig. 3a. However, in the pig there is an initial positive pressure injury in all three regions, followed by a second slight increase in only the cerebrum and cerebellum, and then a final significant increase in only the cerebrum. A similar behavior in the pig is seen with the negative pressure criterion except the order of regions is somewhat reversed, such that the cerebrum and cerebellum only see an initial increase in injury and the brain stem sees three distinct rises in injury. The negative pressure criterion in the human brain only predicts a very small injury that is concentrated in the cerebrum.

The temporal evolution in the brain is nearly identical for all side-on blast overpressure magnitudes under consideration, thus only the injury at the final time is considered for the other blasts in this study. The results of the remaining blasts for the equal charge weight study are shown in Figs. 5 and 6. As expected, the injury in the total brain volume, in both the human and the pig for both the positive and negative pressure criteria, increases with charge weight. For the positive pressure injury, the human brain stem appears to be the region where a small increase in charge weight yields a proportionally larger increase in injury. The injury to the human cerebrum and cerebellum increases almost linearly with charge weight, but in the brain stem, the injured volume progresses from the lowest level of injury to the highest level of injury. In the pig, the brain stem seems to be the most protected region for positive pressure injury, but for negative pressure, it appears to be main driver of total injured volume.

In the equal injury study, equal injury is defined as the overpressure that causes the human and the pig to have the same total injured brain volumes at the end of the analysis within 2% of one another using the 235 kPa injury criteria. The temporal evolution of positive pressure injury for this study is shown in Figs. 7a and 7b, and, as expected from the previous result, the evolution of injury in the pig and human is different. To elicit the same injured volume as the human, the pig had to be subjected to overpressures that were anywhere from 50% to over 100% higher than what the human was subjected to. Subjecting the pig to these pressures only increased the disparity in the negative pressure injury prediction. The injured volumes in the different regions of the brain are shown in Figs. 7c–7f. For the positive pressure injury, the cerebrum and brain stem in the pig and human have

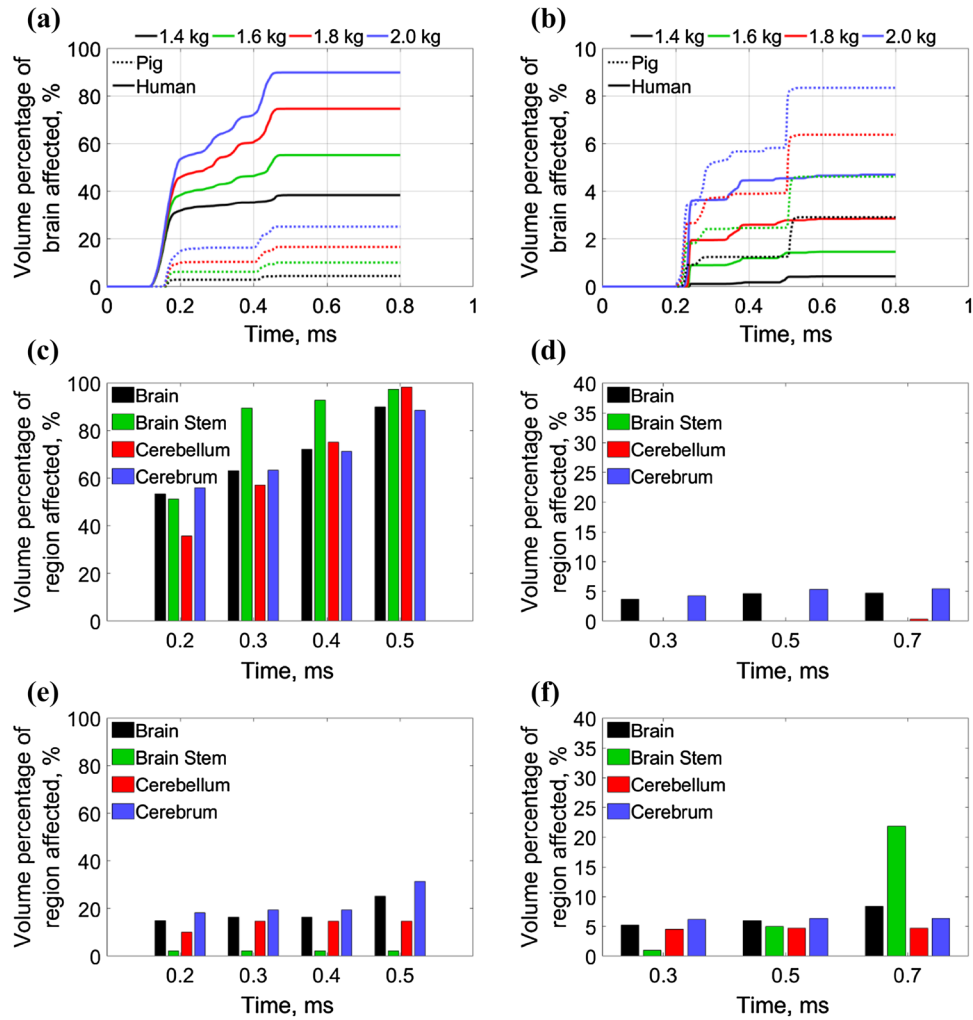


FIGURE 3. Temporal injury in human and porcine for the *equal charge weight study*. (a) 235 kPa injury criterion, (b) – 100 kPa injury criterion; the charge weights are shown on top of the plots. The injured volume percent for the whole brain, cerebrum, cerebellum, and brain stem for 2.0 kg charge weight at discrete time steps are shown in (c) and (d) for the human, and (e) and (f) for the porcine for 235 and – 100 kPa injury criteria, respectively.

almost identical levels of injury. In the cerebellum, the injury is nearly identical between the pig and human at lower equivalent total injured volumes, but at higher total injured volumes the injured cerebellum volume begins to differ. The negative pressure injury shows similar behaviors as seen in Fig. 6, except the pig brain injured volume has now greatly increased.

Lastly, the total injured volume for each injury criterion is plotted against the charge weight for all simulated cases for human and pig in Fig. 8. A linear regression is applied to both types of injuries as a first order approximation of the injury evolution with charge weight. The linear equations describing the pressure injury fits are of the form:

$$V = A \cdot x + B,$$

where V is the injured volume in %, A and B are constants, and x is either the charge weight in kg or the

peak overpressure in kPa. Table 4 lists the constants A and B for the equations describing the positive and negative injury in both human and pig. Note that the constants do not give zero injury at zero charge weight. This is representative of the fact that humans and pigs have some tolerance to blast before becoming injured. These lines can be used to predict the volume of brain injury for a known charge weight or predict the charge weight to cause a known injury volume. Moreover, solving for a given charge weight gives a relationship or, in other words, correspondence rule, between the human injury and pig injury. Therefore, the correspondence rules for the positive injury criterion are:

$$V_{235 \text{ kPa}}^H = 1.8 \cdot V_{235 \text{ kPa}}^P + 31.2$$

for relating injury through charge weight, and

$$V_{235 \text{ kPa}}^H = 1.8 \cdot V_{235 \text{ kPa}}^P + 35.2$$

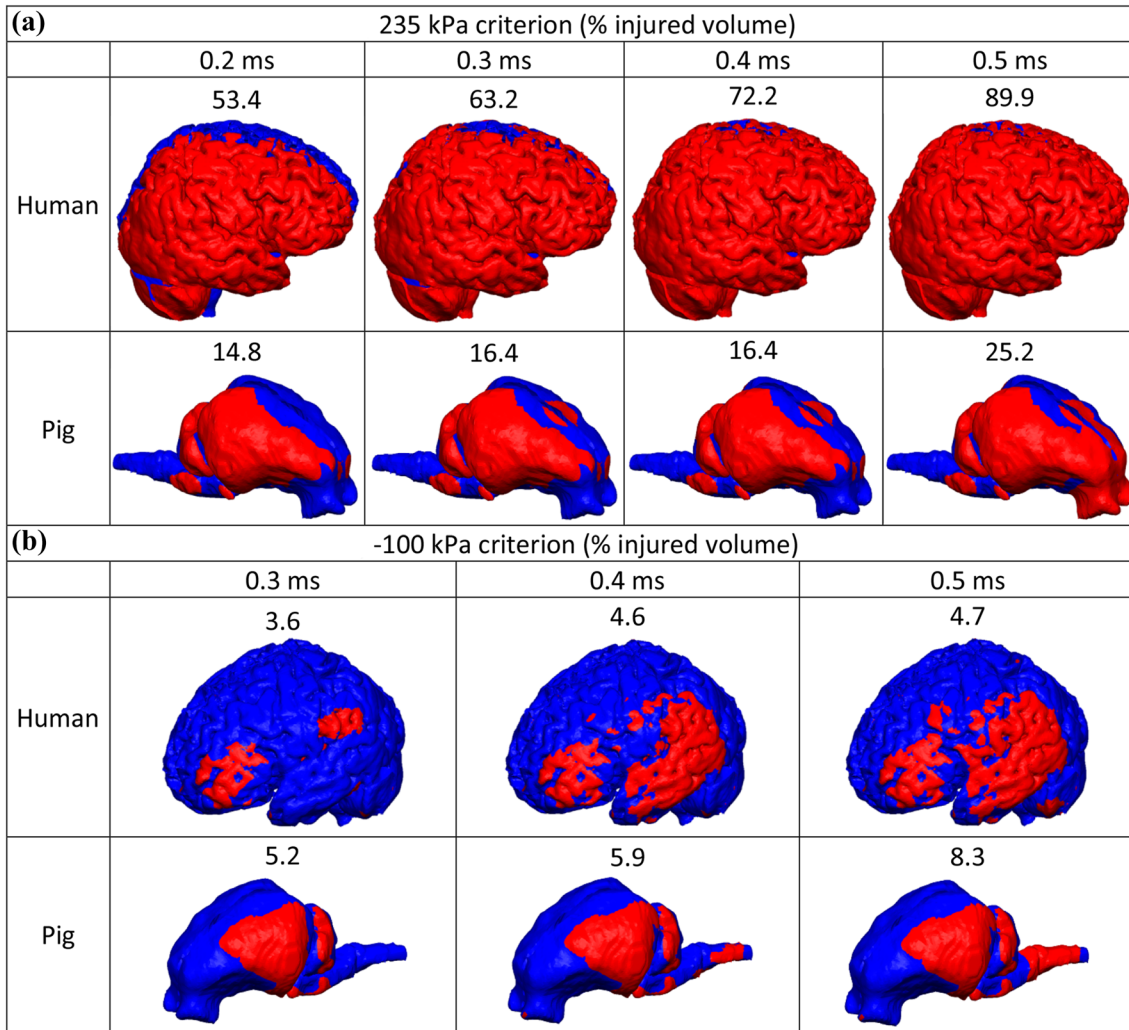


FIGURE 4. Spatial injury results for the 2.0 kg load at various time steps for the duration of the analysis for (a) 235 kPa (brain oriented to show coup injury), and (b) –100 kPa (brain oriented to show counter-coup injury) injury criteria. The red region represent an injured region. (a) Top row corresponds to Fig. 3c and bottom row corresponds to Fig. 3e. (b) Top row corresponds to Fig. 3d and bottom row corresponds to Fig. 3f.

for relating injury through peak overpressure; and for the negative injury criterion, it is:

$$V_{-100 \text{ kPa}}^H = 0.79 \cdot V_{-100 \text{ kPa}}^P - 1.92$$

for relating injury through charge weight, and

$$V_{-100 \text{ kPa}}^H = 0.81 \cdot V_{-100 \text{ kPa}}^P - 2.38$$

for relating injury through peak overpressure, where V^H represent the human brain injured volume in % and V^P represents the pig brain injured volume in %.

DISCUSSION

The temporal evolution of injury, Figs. 3 and 7, shows that even though injured volumes may be different, the evolution over time appears to exhibit

similar patterns and similar locations for the human and the pig. The positive pressure injury has a clear tendency to develop in the temporal lobe initially and evolve medially to the other lobes. This is a function of the initial peak pressure pulse traversing through and injuring the brain. The prediction of a non-linear increase in injury with time is attributed to the geometry of the subjects' skulls and the complex pressure wave interaction and interference between the brain and skull. Even after the pressure front passes, the reflected in-phase pressure waves may coincide and constructively interfere with each other, which could result in a pressure higher than the threshold at certain locations and thus cause additional injury in the brain.

Subjecting both the pig and human to equal charge weights yielded significant differences in predicted total brain volume injured but similar patterns and evolu-

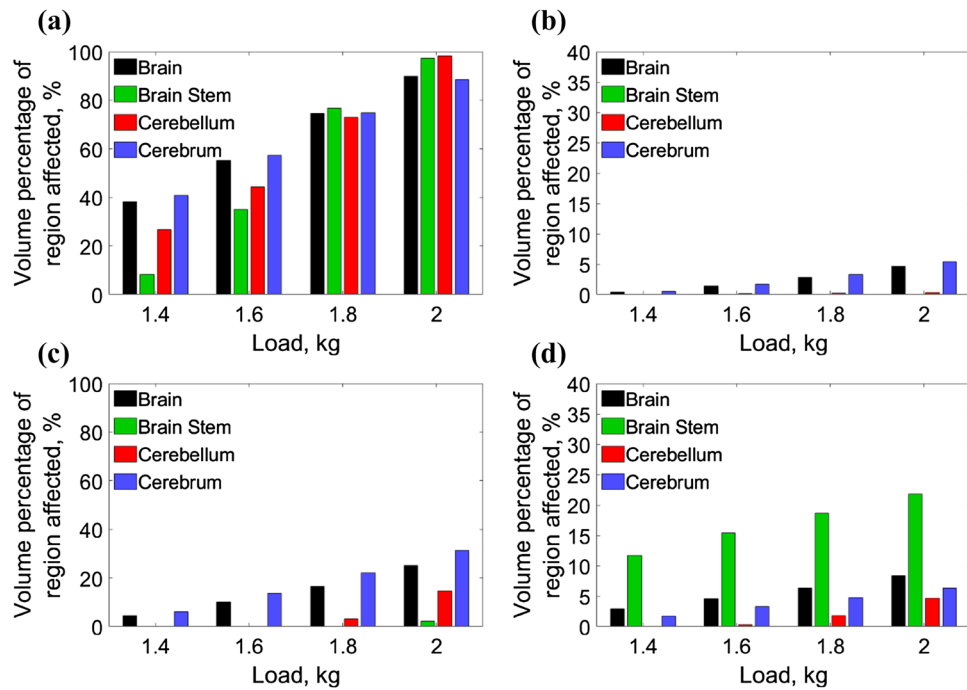


FIGURE 5. (a) Human and (c) pig positive pressure injury and (b) human and (d) pig negative pressure injury results for the *equal charge weight study*. The injured volume in percent is shown for the cerebrum, cerebellum, brain stem, and total brain at the final time of the analysis.

tions of injury were seen. First, it can be noted from Fig. 5 that the human had a higher predicted injury using the positive pressure criteria while the pig had a higher predicted injury with the negative pressure criteria. This indicates that the pig and human geometries are sufficiently different to influence the total injured volume but not so different that they do not experience similar injury patterns. The human brain appears to be more vulnerable to coup (positive pressure) injuries relative to the pig (Fig. 6a), which is more vulnerable to counter-coup (negative pressure) injuries (Fig. 6b). When examining absolute injured volumes though, the pig has much less variability than the human when comparing coup vs. counter-coup vulnerability. While the pig does show more positive pressure injury than negative pressure injury, the values are much closer—a factor of approximately 2–3 depending on the load—than they are in the human, which shows about twenty times as much positive pressure injury than negative pressure injury.

Analyzing only with the positive pressure criterion with equal charge weights, some similarities can be noted between the human and the pig. For example, the highest levels of injury develop first in the cerebrum for both subjects, which is likely a result of the cerebrum being closest to the blast. The negative pressure injury results also show some degree of similarity between the species. The total injured brain volume for human for 1.8 and 2.0 kg charge weights are nearly

identical to those for the pig for the 1.4 and 1.6 kg charge weights, respectively. However, further inspection shows that, under the conditions where equal total injured volume has occurred, the regions where the injury develops to achieve the same equal volume of injury overall are dissimilar between the species. The human brain primarily shows injury in the cerebrum whereas the pig brain primarily shows injury in the brain stem but additional injury is seen in the cerebrum too. This finding indicates that the total injured volume may not always provide a complete picture for building correspondence rules. These differences in injury location could be a significant factor in how the injury is diagnosed in a behavioral study and this fact must be considered when attempting to build correspondence rules.

When comparing equal total injured volumes (Fig. 7), it is first noted that equal injury specified for the 235 kPa criterion does not lead to equal injury for the –100 kPa criterion. This result indicates that a correspondence rule may only be applicable to a specific criterion, which is confirmed by the development of two separate rules for the positive pressure and negative pressure criteria (Fig. 8). This observation also implies that there is no reason to expect that inter-species TBI correspondence rules for one type of loading, e.g., blast overpressure, will be applicable to other types of loading, e.g., blunt or ballistic impact.

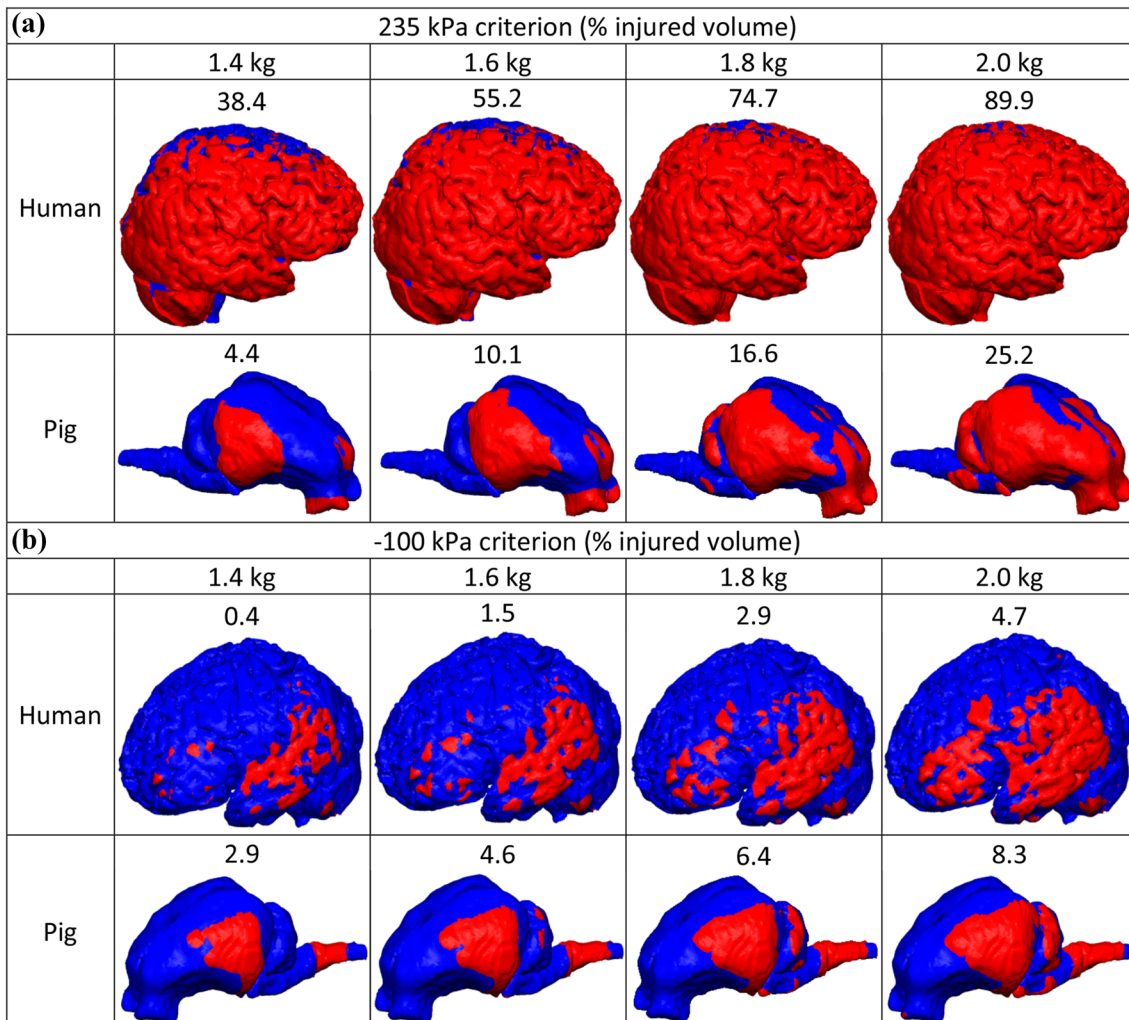


FIGURE 6. Spatial injury results for the equal charge weight study at the final time of the analysis for (a) 235 kPa (brain oriented to show coup injury), and (b) -100 kPa (brain oriented to show counter-coup injury) injury criteria. The red region represent an injured region. (a) Top row corresponds to Fig. 5a and bottom row corresponds to Fig. 5c. (b) top row corresponds to Fig. 5b and bottom row corresponds to Fig. 5d.

The bulk constitutive behavior in biological materials, in general, is nearly incompressible and/or linear whereas the shear behavior can be non-linear and rate dependent. The exposure of the head to a blast overpressure gives rise to an immediate bulk response in the brain with limited contribution from the rate-dependent shear behavior, which is postulated to be the primary cause of TBI due to blunt impacts.²⁸ Thus, the distinct possibility that the mechanisms of bTBI and blunt-impact TBI are fundamentally different would dictate that the correspondence rules for various loading types be exclusive. This can be ascertained by conducting blunt impact simulations and verifying whether both shear- and pressure-based injury predictions follow the same pressure-based correspondence rules developed in this study.

The original data and the curve fits in Fig. 8 provide a useful set of pressure-based injury correspondence rules. With further improvements and extended validation, the pig FE model could be replaced with a live subject and these correspondence rules could be used to directly relate the TBI caused in the pig from blast testing to TBI in a human for the same charge weight. With the accumulation of more data using different charge weights, standoff distances, and subject orientations, the developed correspondence rules can be generalized to create a response surface to predict TBI in humans for a much broader range of blast overpressures. Additionally, the developed correspondence rules can be further extended to other types of loading, such as blunt impact, where they can still be exploited for pressure-based TBI, in addition to exclusive shear-

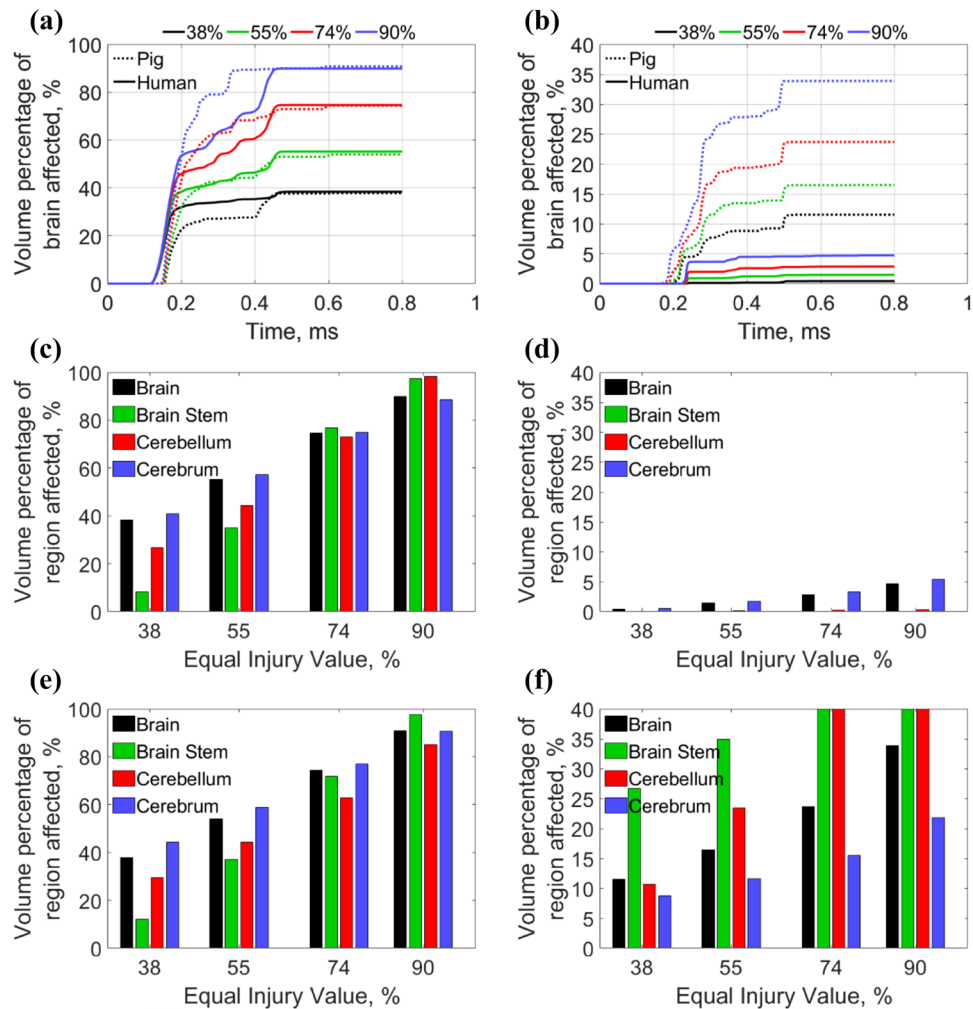


FIGURE 7. Temporal injury results in the pig and human for the *equal injury study*. (a) 235 kPa injury criterion, (b) – 100 kPa injury criterion; the percentages of total injured volumes at the end of the analysis are shown on top of the plots. The injured volume percent for the whole brain, cerebrum, cerebellum, and brain stem for *equal injury study* are shown in (c) and (d) for the human, and (e) and (f) for the porcine for 235 and – 100 kPa injury criteria, respectively.

based correspondence rules applicable for blunt impact only.

The correspondence rules developed here are different from traditional scaling rules that relate injury to mass, time, geometry, or material behavior. The rules developed in this study directly related a predicted injury in one species (pig) to the predicted injury in another species (human) through the input parameter, charge weight or peak pressure, which causes the injury. In relating predicted injury in this fashion, the material behavior, geometry, and mass are implicitly considered, whereas the time need not be scaled since the blast insults are identical on both subjects.

The development of correspondence rules in this work should be understood with the following considerations and limitations: (1) The use of traditional (linear) 4-node tetrahedral element can lead to volumetric locking and suppress the development of shear

modes of deformation. To overcome this phenomenon, a modified four-node tetrahedral element formulation based on the average of the nodal pressures² has been used to develop the FE models in this study. The reader is referred to the work of Bonet *et al.*³ on the comparative performance of the modified tetrahedral element and other 4-node elements. Furthermore, the accuracy and mesh convergence characteristic of these elements were benchmarked by comparing the simulation results of the blast loading of an idealized skull-brain complex with the commonly used linear 8-node brick element and quadratic, 10-node tetrahedral element.²¹ The best practice would be to benchmark these elements every time there is a notable change in the constitutive models and/or loading conditions. (2) As per accepted practice, the porcine and human brain tissue properties have been assumed to be the same. An evidence-based change in this material correlation may

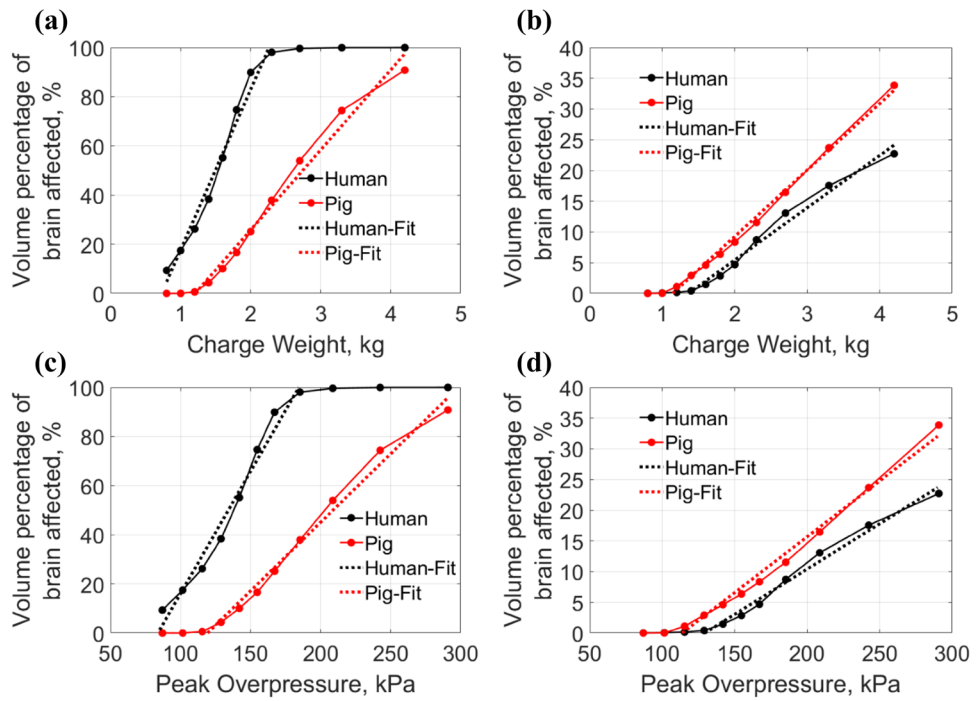


FIGURE 8. Volumetric injury results plotted against explosive charge weight (a and b) and peak overpressure (c and d) used for the human and porcine models: (a and c) 235 kPa injury criteria, (b and d) – 100 kPa injury criteria. The coefficients used in the linear equations describing the pressure injury fits are shown in Table 4.

TABLE 4. Constants used to describe the linear regression relating injured volume to charge weight and peak overpressure.

	A (%/kg, %/kPa)	B (%)
235 kPa pressure criteria		
Human	65.2, 0.994	- 47.4, - 83.3
Pig	32.6, 0.558	- 39.3, - 66.5
– 100 kPa pressure criteria		
Human	8.51, 0.147	- 11.6, - 19.1
Pig	10.8, 0.182	- 12.3, - 20.7

affect the correspondence rules. The same will be true for advances in the characterization of the complex behavior of brain tissue under high rate of deformation conditions. (3) The ConWep blast wave model works well within the range of scaled distances in open field conditions considered here; however, it becomes less accurate when multiple wave reflections and diffraction are involved, or when there are areas of stagnation and other complex effects. (4) As mentioned earlier, the exact mechanisms of bTBI are an active area of research. Given the many biomechanical thresholds of injury suggested in the literature, the pressure-based biomechanical thresholds have been used in this study for several factors; most notably among them is the absence of large strains in the blast event. However, it is possible that more definitive research in the future could show otherwise and lead to modification of the

correspondence rules developed here. Which also makes it potentially possible that some of the inactive thresholds not given consideration in this work (see Table 2) may become relevant. (5) The correspondence rules do not conform to allometric scaling that is commonly used to correlate biological data across species; for example, Rafaels *et al.*¹⁸ have developed allometric scaling for mild TBI based on experiments on ferrets. Basically, it suggests that for the pressure-based criteria, scaling with mass and other geometric and morphological measures was not obtained between the pig and human subject in this study. However, this does not contradict the utility of the correspondence rules as described above in the discussion of results. (6) The correspondence rules correlate predicted injury between pig and human, but they do not reflect on the degree of severity of the injury because they are injury location independent. For example, a 5% injury in the frontal cortex is treated the same way as a similarly proportioned injury in the brain stem.

In summary, the two types of case studies conducted in this paper have laid the basis for the development of interspecies (human–porcine) correspondence rules for bTBI. The results have reinforced the notion that barring experimental evidence for a shear-based mechanism or a yet unknown mechanism altogether, currently only pressure-based criteria can be used to

describe “injury” under blast overpressure loading. Next, it was demonstrated that the pig and the human do not experience blast the same way. The regions of the brain that become injured and predicted injured volumes are different for both the positive and negative pressure injury criteria, with the same charge weights applied to the models. It was also shown that blast loads from different charge weights could produce the same total injured volume for a given threshold for both the pig and the human, but the regions where injury occurs and injured volumes in those regions would not necessarily be the same for the pig and the human. At the same time, the injured volume equality would not hold when applied to other injury metrics. However, if the spatial and temporal variations are neglected in favor of total injured volume as the metric, then correspondence can be created between human and pig bTBI, as evidenced by the two sets of rules derived here. Ongoing work is focused on generating more data to refine these correspondence rules as well as to determine their applicability for different standoff distances as well as blast orientations.

ACKNOWLEDGMENTS

This work was supported by the Office of Naval Research (ONR) under contract number N001415WX00531 and the Department of Defense (DoD) High Performance Computing Modernization Program (HPCMP) using the Air Force Research Laboratory (AFRL) and U.S. Army Corps of Engineers Research and Development Center (ERDC) Major Shared Resource Center (MSRC) under project 416, subproject 572. The authors acknowledge Dr. Ross Cotton from Simpleware® for the generation of the human head FE meshes. The authors acknowledge Dr. Tim Bentley from ONR for his support and technical discussions as well as Dr. Thomas O’Shaughnessy from NRL for technical discussions. The authors also acknowledge Drs. Kirubel Teferra and Patrick Brewick for their revisions and feedback. SMQ acknowledges the support of the National Science Foundation under the Internal Research & Development Program.

REFERENCES

- ¹Bass, C. R., M. B. Panzer, K. A. Rafael, G. Wood, J. Shridharani, and B. Capehart. Brain injuries from blast. *Ann. Biomed. Eng.* 40:185–202, 2012.
- ²Bonet, J., and A. J. Burton. A simple average nodal pressure tetrahedral element for incompressible and nearly incompressible dynamic explicit applications. *Commun. Numer. Methods Eng.* 14:437–449, 1998.
- ³Bonet, J., H. Marriott, and O. Hassan. Stability and comparison of different linear tetrahedral formulation for nearly incompressible explicit dynamic applications. *Int. J. Numer. Methods Eng.* 50:119–133, 1998.
- ⁴Brewick, P., R. Saunders, and A. Bagchi. Biomechanical modeling of the human head. NRL/FR/6350-17-10304. Washington, DC: Naval Research Laboratory, Defense Technical Information Center, 2017. www.dtic.mil/docs/citations/AD1040988.
- ⁵Brewick, P., and K. Teferra. Uncertainty quantification for constitutive model calibration of brain tissue. *J. Mech. Behav. Biomed. Mater.* 2018. <https://doi.org/10.1016/j.jmbm.2018.05.037>.
- ⁶Cernak, I. Animal models of head trauma. *NeuroRx.* 2:410–422, 2005.
- ⁷Cotton, R. T., C. W. Pearce, P. G. Young, N. Kota, A. C. Leung, A. Bagch, and S. M. Qidwai. Development of a geometrically accurate and adaptable finite element head model for impact simulation: the Naval Research Laboratory-Simpleware Head Model. *Comput. Methods Biomed. Eng.* 19(1):101–113, 2016.
- ⁸Courtney, A., and M. Courtney. The complexity of biomechanics causing primary blast-induced traumatic brain injury: a review of potential mechanisms. *Front. Neurol.* 6:221, 2015.
- ⁹Deck, C., and R. Willinger. Improved head injury criteria based on head FE model. *Int. J. Crashworthiness* 13(6):667–678, 2008.
- ¹⁰Deck, C., and R. Willinger. The current state of the human head finite element modelling. *Int. J. Veh. Saf.* 4:85–112, 2009.
- ¹¹Jean, A., M. K. Nyein, J. Q. Zheng, D. F. Moore, J. D. Joannopoulos, and R. Radovitzky. An animal-to-human scaling law for blast-induced traumatic brain injury risk assessment. *Proc. Natl. Acad. Sci.* 111:15310–15315, 2014.
- ¹²Johnson, V. E., D. F. Meaney, D. K. Cullen, and D. H. Smith. Animal models of traumatic brain injury. *Handb. Clin. Neurol.* 127:115–128, 2015.
- ¹³Kang, H. S., R. Willinger, B. M. Diaw, and B. Chinn. Validation of a 3D anatomic human head model and replication of head impact in motorcycle accident by finite element modeling. *SAE Techn. Pap.* 41:315–325, 1997.
- ¹⁴Kingery, C. N. Air-blast parameters from TNT spherical air burst and hemispherical surface burst. Aberdeen Proving Ground, MD: Army Ballistic Research Lab, Defense Technical Information Center, 1966. [https://urldefense.proofpoint.com/v2/url?u=http-3A-www.dtic.mil_dtic_tr_fulltext_u2_811673.pdf&d=DwICAg&c=vh6FgFnduejNhP_PDOfl_yRaSfZy8CWbWnIf4XJhSqx8&r=cijxKIUffjh6xB3_5XSxKelnSNfz2185wGO_qFr-DFH8&m=8TeaFt318zTatWYkxpH4Hft8WVAkx79q-zVm5PIH5u4&s=aK8p4jB1t_swV_dL4RswcKs2eFhrzuPdQknmcF_Yh-Y&e=.](https://urldefense.proofpoint.com/v2/url?u=http-3A-www.dtic.mil_dtic_tr_fulltext_u2_811673.pdf&d=DwICAg&c=vh6FgFnduejNhP_PDOfl_yRaSfZy8CWbWnIf4XJhSqx8&r=cijxKIUffjh6xB3_5XSxKelnSNfz2185wGO_qFr-DFH8&m=8TeaFt318zTatWYkxpH4Hft8WVAkx79q-zVm5PIH5u4&s=aK8p4jB1t_swV_dL4RswcKs2eFhrzuPdQknmcF_Yh-Y&e=)
- ¹⁵Kleiven, S. Predictors for traumatic brain injuries evaluated through accident reconstructions. *Stapp Car Crash J.* 51:401–435, 2007.
- ¹⁶Margulies, S. S., and L. E. Thibault. A proposed tolerance criterion for diffuse axonal injury in man. *J. Biomech.* 25(8):917–923, 1992.
- ¹⁷Panzer, M. B., G. W. Wood, and C. R. Bass. Scaling in neurotrauma: How do we apply animal experiments to people? *Exp. Neurol.* 261:120–126, 2014.
- ¹⁸Rafael, K. A., C. R. Bass, M. B. Panzer, R. S. Salzar, W. A. Woods, S. H. Feldman, T. Walliko, R. W. Kent, B. P.

- Capehart, J. B. Foster, B. Derkunt, and A. Toman. Brain injury risk from primary blast. *J. Trauma Acute Care Surg.* 73(4):895–901, 2012.
- ¹⁹Saunders, R., N. Kota, A. Bagchi, and S. Qidwai. On challenges in developing a high-fidelity model of the human head for traumatic brain injury prediction. NRL/MR/6350-18-9807. Washington, DC: Naval Research Laboratory, Defense Technical Information Center, 2018. https://urldefense.proofpoint.com/v2/url?u=http-3A-www.dtic.mil_dtic_tr_fulltext_u2_1063014.pdf&d=DwICAg&c=vh6FgFnduejNhPPD0fl_yRaSfZy8CWbWnIf4XJhSqx8&r=cijxKIUfljh6xB35XSxKelnSNfz2185wGO_qFr-DFH8&m=DZXI9-X7q9mk3hA93vZMA8uoihLUXzP6YyTtijv5Cqg&s=knbg6Lvdq9UdhpUkUFQV2iDcyDnojJyebQWyYcRL7x0&e=.
- ²⁰Takhounts, E. G., R. H. Eppinger, J. Q. Campbell, and R. E. Tannous. On the development of the SIMon finite element head model. *Stapp Car Crash J.* 47:107–133, 2003.
- ²¹Tan, X. G., M. M. D’Souza, S. Khushu, R. K. Gupta, V. G. DeGiorgi, and A. K. Singh. Computational modeling of blunt impact to head and correlation of biomechanical measures with medical images. In: Proceedings of the ASME 2018 International Mechanical Engineering Congress & Exposition. Paper No. 88026, 2018.
- ²²Tan, X. G., A. J. Przekwas, and R. K. Gupta. Computational modeling of blast wave interaction with a human body and assessment of traumatic brain injury. *Shock Waves* 27(6):889–904, 2017.
- ²³Tan, X. G., R. N. Saunders, and A. Bagchi. Validation of a full porcine finite element model for blast induced TBI using a coupled Eulerian-Lagrangian approach. In: Proceeding of the ASME 2017 International Mechanical Engineering Congress & Exposition, pp. V003T04A035–V003T04A035, 2017.
- ²⁴Teferra, K., X. G. Tan, A. Illiopoulos, J. Michopoulos, and S. Qidwai. Effect of human head morphological variability on the mechanical response of blast overpressure loading. *Int. J. Numer. Method. Biomed. Eng.* 2018. <https://doi.org/10.1002/cnm.3109>.
- ²⁵Thibault, K. L., and S. S. Margulies. Age-dependent material properties of the porcine cerebrum: effect on pediatric inertial head injury criteria. *J. Biomech.* 31(12):1119–1126, 1998.
- ²⁶Wright, R. M., and K. T. Ramesh. An axonal strain injury criterion for traumatic brain injury. *Biomech. Model. Mechanobiol.* 11(1–2):245, 2012.
- ²⁷Young, P. G., T. B. Beresford-West, S. R. Coward, B. Notarberardino, B. Walker, and A. Abdul-Aziz. An efficient approach to converting three-dimensional image data into highly accurate computational models. *Philos. Trans. R. Soc. Lond. A* 366(1878):3155–3173, 2008.
- ²⁸Zhang, L. KH Yang, AI King. Biomechanics of neurotrauma. *Neurol. Res.* 23(2–3):144–156, 2001.
- ²⁹Zhang, L., K. H. Yang, and A. I. King. A proposed injury threshold for mild traumatic brain injury. *J. Biomech. Eng.* 126(2):226–236, 2004.
- ³⁰Zhu, F., C. C. Chou, K. H. Yang, and A. I. King. Some considerations on the threshold and inter-species scaling law for primary blast-induced traumatic brain injury: a semi-analytical approach. *J. Mech. Med. Biol.* 13(04):1350065, 2013.